



HAL
open science

High efficiency Step-Up HVDC converter for photovoltaic generator

Jean-Paul Sawicki, Pierre Petit, Abdallah Zégaoui, Michel Aillerie,
Jean-Pierre Charles

► To cite this version:

Jean-Paul Sawicki, Pierre Petit, Abdallah Zégaoui, Michel Aillerie, Jean-Pierre Charles. High efficiency Step-Up HVDC converter for photovoltaic generator. Terragreen 12 Clean Energy Solutions for Sustainable Environment, Feb 2012, Beyrouth, Lebanon. hal-01234154

HAL Id: hal-01234154

<https://hal.science/hal-01234154>

Submitted on 10 Dec 2020

HAL is a multi-disciplinary open access archive for the deposit and dissemination of scientific research documents, whether they are published or not. The documents may come from teaching and research institutions in France or abroad, or from public or private research centers.

L'archive ouverte pluridisciplinaire **HAL**, est destinée au dépôt et à la diffusion de documents scientifiques de niveau recherche, publiés ou non, émanant des établissements d'enseignement et de recherche français ou étrangers, des laboratoires publics ou privés.

TERRAGREEN-LB 2012

High efficiency Step-Up HVDC converter for photovoltaic generator

Jean-Paul Sawicki^a, Pierre Petit^a, Abdallah Zégaoui^{a,b}, Michel Aillerie^a,
and Jean-Pierre Charles^a

^a*LMOPS, University of Lorraine and Supélec, 2 rue Edouard Belin, 57070 Metz, France.*

^b*University Hassiba Ben Bouali, BP 154, 02000 Chlef, Algeria.*

jsawicki@univ-metz.fr, aillerie@metz.supelec.fr

Abstract

Nowadays a way to optimize photovoltaic systems consists in implementing distributed structures, implying the use of electronic devices. In this paper we show performances of improved DC-DC converters able to feed an inverter. Resulting efficiency allow us to consider parallel HVDC architecture connecting independently PV modules with low section wiring.

Keywords: Photovoltaic; DC/DC converter; MOSFET; Step-Up.

1. Introduction

Photovoltaic energy doesn't fluctuate only because of natural drops of sunshine (clouds, bad weather, variable length of day according to the seasons...), or human activity as industrial pollution [1] but also because of shadowing of PV arrays due to vegetation or surrounding obstacles (chimneys, voltage lines, buildings...)[2].

To take into account first disturbances classical approach consists in maximum point of power tracking (MPPT) owing to algorithms implemented in inverters (grid connected systems), in advanced charge controllers (storage in battery) and in micro-inverters or DC-DC converters [3] directly connected to the modules in distributed structures.

For the second type of disturbances static solutions as bypass diodes were first purposed to protect the part of module exposed to shadows without preventing noticeable impact on classical string energy output. But, as for the first case, the choice to connect electronic device to the modules exposed to

shadowing is considered as a serious way to increase PV system efficiency. So three kinds of industrial solutions can be encountered:

- micro-inverters directly generating AC grid voltage, whose first developments date from the beginning of the nineties,
- more recently, power optimizers used in conventional DC high voltage strings of modules connected to conventional or specific central inverters,
- an electronic box controlling multi-lane module layout able to disconnect weak modules from a virtual string supplying a central inverter.

The first approach allows (non exhaustive list) a reduction of components, like junction boxes, DC connectors, bypass (if single in the module) and blocking diodes, DC fusing over-current and DC surge protection, with cheaper wiring as a bonus. Another additional advantage consists in safety improvement: this architecture reduces significantly arc faults because there is no DC high voltage anymore and one can easily stop all the inverters, as example in case of firemen interventions. At this time, PV modules with micro-inverter are rather set up in residential area, with monitoring of few tens modules. But such kinds of panels can be directly connected to voltage lines in streets, for example to sustain grid. Thanks to parallel architecture, one or more shaded modules don't disturb the others and they can be separately and automatically disconnected without stopping all the system.

The second approach tries to connect working modules in an independent configuration in spite of the series configuration: such uncoupling is realized by using individual MPPTs, which increase the DC-DC ratio of the converter individually connected to a PV module. Except in case of shading risks, as example, it is not necessary to install these optimizers in all the strings. In this way, ancient systems can easily be improved to increase power harvest. As a variant we can find also a specific solution supplying fixed voltage of the string, in the limit of adjustment of every module in case of disturbances like partial shadows. Main advantage consists in using a simplified inverter supplied by its best efficiency voltage not needing its own MPPT.

The last architecture concentrates all the interconnections between modules in one electronic device: the best configuration of string to optimize power harvest is chosen in real time but main drawback consists in noticeable growth of wiring length.

Every of these three architectures allow precise monitoring of each module integrating a converter, improving availability of installation, owing to an easier fault diagnosis.

2. DC voltage bus

2.1. Parallel architecture

Keeping in mind that DC converters are simpler and less expensive than inverters we can imagine designing a boost step-up connected to each module and able to supply a string inverter with its best efficiency voltage (Fig 1).

Parallel architecture with common voltage allows also connection between different kinds of modules: for example amorphous silicon modules, good for diffuse light, associated with mono-crystalline or polycrystalline silicon, efficient for direct sunshine.

Different power modules are able to work simultaneously and it is consequently possible to purpose an installation of modules on a same roof whose faces don't benefit of the same sunshine (north, east, south and west faces), when keeping only one inverter connected to grid. So, parallel layout is particularly convenient for minimizing shadowing effects. Moreover, thanks to higher voltage supplied by every converter, cable section can decrease strongly, what is financially interesting, and there is no impedance problem with great wiring lengths any more, unlike AC voltage.

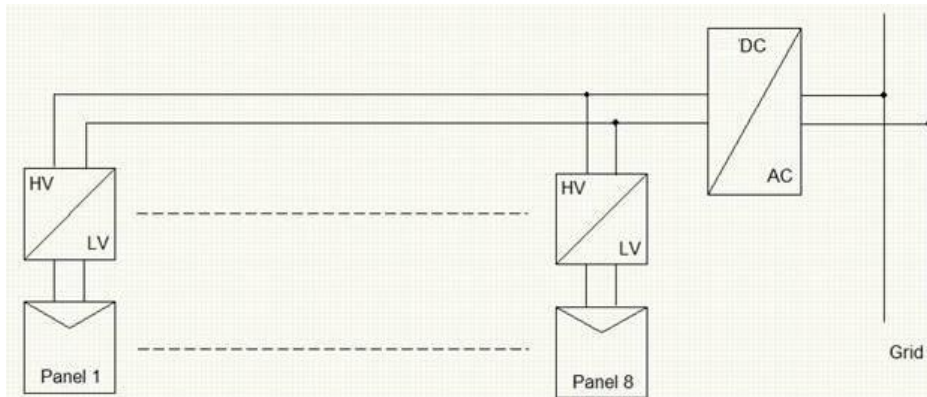


Fig 1: schematic representation of a distributed photovoltaic generator built with 8 PV panels associated with dc/dc converters connected via an inverter to the grid.

2.2. Improved step-up structures.

In this paper we will expose results of studies improving DC step up converter able to reach the best efficient voltage.

Previously we have studied the limitations of a classical boost step up, particularly losses due to MOSFET $R_{ds(on)}$ (resistance between source and drain during conduction) preventing to obtain efficient high voltages. Principal results have been submitted in another paper [4]. In brief, this structure is not suitable for voltage higher than hundred volt, insufficient value to supply classical inverters. Indeed, higher voltages need asymmetrical duty cycle, disastrous for efficiency of DC converter.

In a second time we have imagined to add a second self strongly magnetically coupled to the first (Fig 2), as used in high voltages supplying cathodic ray tube. But the main drawback consist in parasitic oscillations on MOSFET drain, with a voltage between drain and source similar to this of output converter, leading to use a switch with an high $R_{ds(on)}$ and as consequences a drastic increase of losses and a significant drop of converter performances.

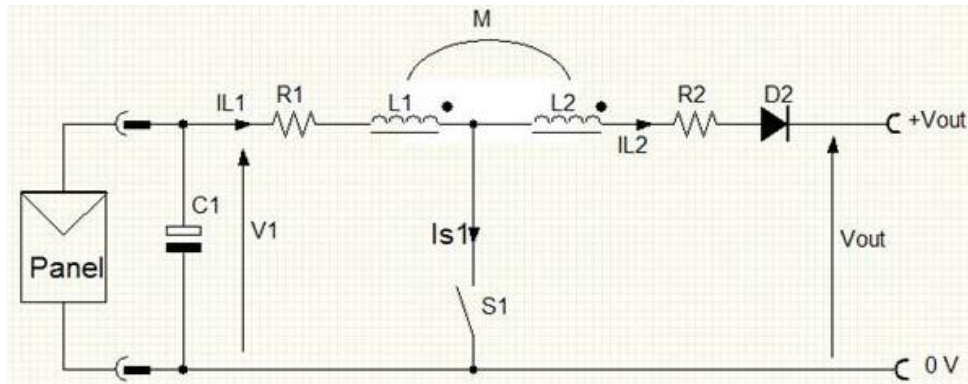


Fig.2: electronic diagram of the ideal double coils boost converter. The MOSFET transistor, S_1 , is connected at the middle of two magnetically coupled inductors.

In order to limit the overvoltage on the drain of the power MOSFET and to insure energy recovery, we modified the previous structure by introducing a diode D_1 , and a capacitor C_3 in order to store and transmit in the output stage all energy available on the MOSFET drain (Fig. 3). This electronic structure, we will name Magnetically Coupled Boost (MCB), was earlier purposed for various applications [5], and in photovoltaic area with supplementary components as capacitors and diodes [6].

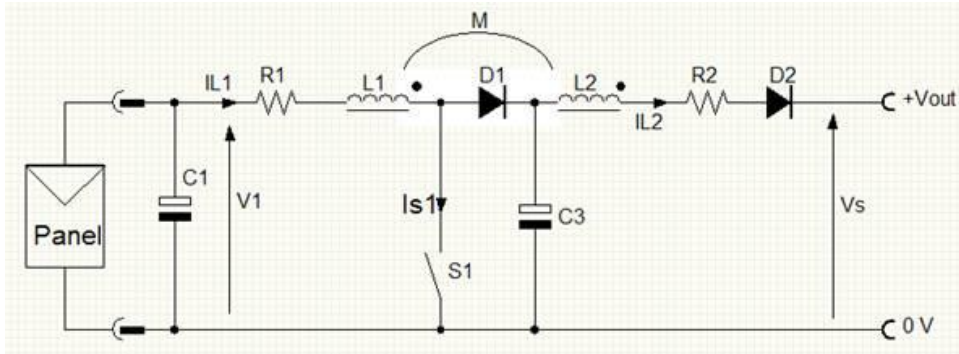


Fig 3: electronic diagram of the ideal magnetically coupled boost DC-DC converter with recovery stage.

Thus, this structure is composed by an input stage, usually named Step-Up stage followed by a recovery stage whose role is to increase the voltage in the recovered energy phase.

2.3. Simulations

The real circuit, i.e. with all parasitic elements neglected previously is represented in Fig. 4.

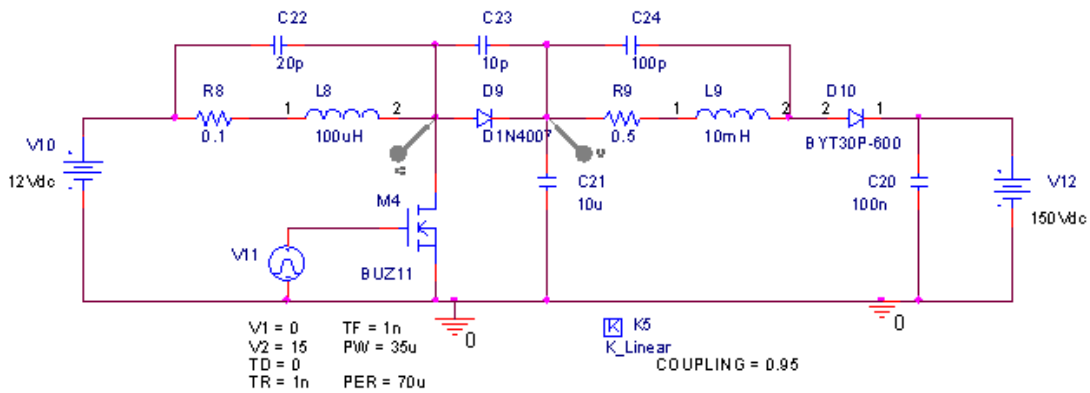


Fig.4: electronic diagram of the real magnetically coupled coils boost converter with recovery stage.

C_{22} and C_{24} are equivalent to capacitances in the primary and secondary coils, respectively while C_{23} is the parasitic capacitance between the two coils. We have started ORCAD simulations with this setup; the chronograms are reported in Fig. 5.

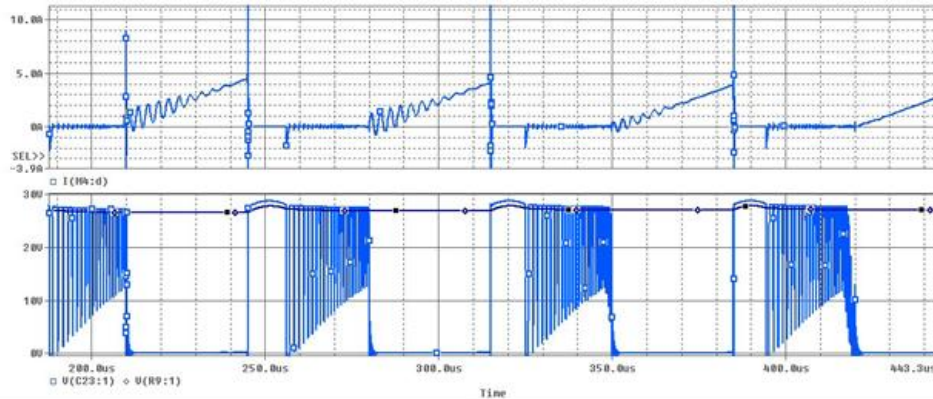


Fig. 5: chronograms of current and voltage in the magnetically coupled boost converter with recovery stage.

I_{M4} is MOSFET current when conducting state, V_{C23} is equivalent to MOSFET drain voltage and V_{R9} is the output voltage of D_9 diode. There is no over-voltage on the MOSFET like appeared in converter without diode recovery stage, which is interesting for the choice of a low R_{dson} , but noticeable oscillations are present when blocking the switch.

This phenomenon is due to the output parasitic capacitances (diode D_{10} , C_{23} , and C_{24}) and rises with the voltage transformation ratio. We have used a ratio equal to 10 (ratio of 100 between L_8 and L_9 inductances). The expected output voltage is about 150V to 200V for an input voltage about 12V. For higher output voltages we must increase the turns of the transformer secondary coil, implying a greater incidence of the output parasitic capacitances. Simulation values of parasitic capacitances have been successively neared to correspond with the frequency of the pseudo oscillations when experimenting MCB converter (Fig. 6).

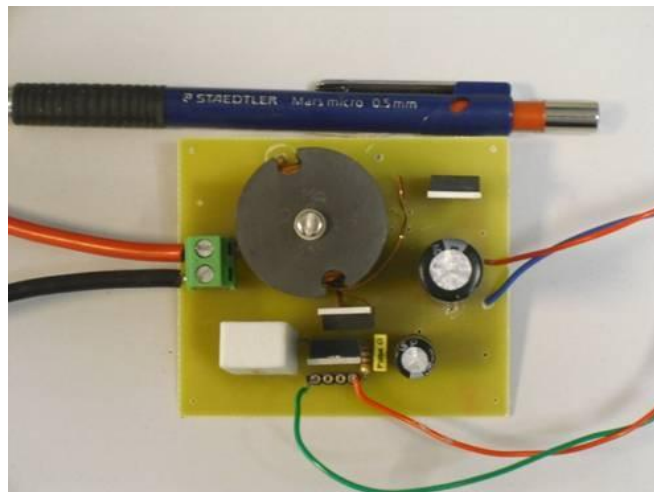


Fig 6: picture of magnetically coupled boost converter prototype.

In this picture we clearly show the autotransformer, realized with a N22 Siemens ferrite core, the capacitors, the MOSFET (IRF2807 reference, with $R_{dson} = 13\text{m}\Omega$, $V_{dsmax} = 75\text{V}$, $I_{dmax} = 82\text{A}$, input

capacitance $C_{iss} = 3820$ pF) and the diodes, particularly Si carbide recovery diode, D9 in Fig. 5 (NF8486 reference, with reverse voltage $V_r = 600$ V).

So, a few components are different between simulation and prototype:

- The implemented MOSFET was not available when computing. It has been chosen later for its improved electrical specifications,
- There was no recovery Si carbide diode model in ORCAD, which explains conventional diode.

2.4. Experiments.

We report the recording traces of the output voltage, V2, the drain-source voltage of the MOSFET, Vds, the source current, Is and the control signal of the MOSFET for two switching frequencies, 27 kHz and 47 kHz, in Figs. 7.a and 7.b, respectively. The acquisition of the source current has been done on an oscilloscope by insertion of a 0.22Ω resistor, keeping in mind, nevertheless, this method introduces joule losses decreasing the global efficiency.

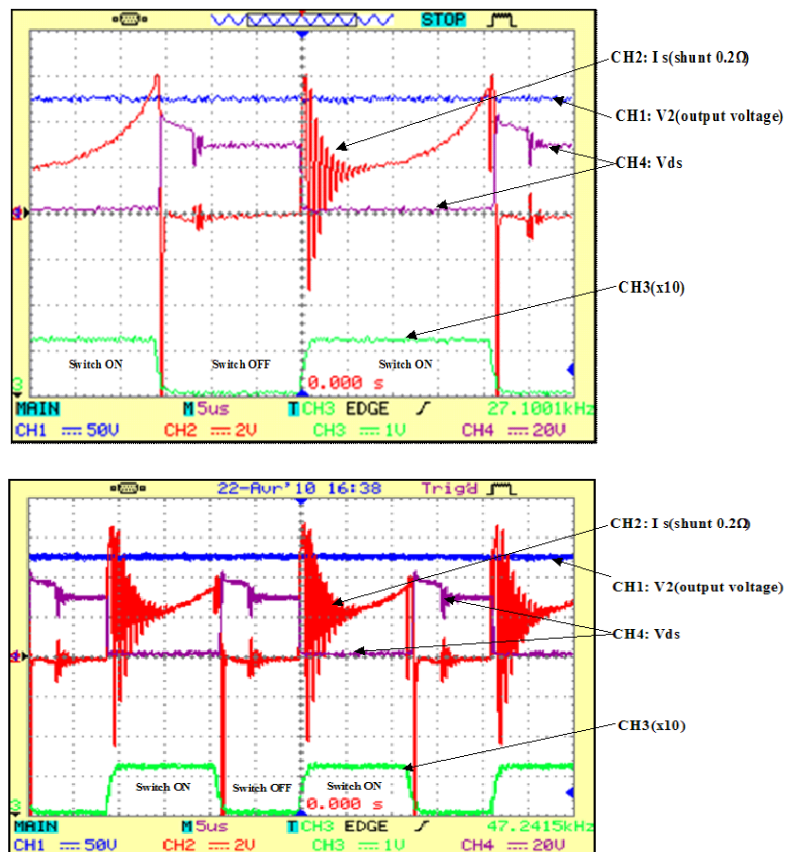


Fig. 7: experimental oscillograms obtained with two switching frequencies (a) 27 kHz, (b) 47 kHz. CH1: Step-Up V2 (output voltage), CH2: Is (voltage on a 0.22Ω shunt), CH3(x10): Switch ON=12V, Switch Off=0V, CH4: V_{DS} voltage.

We can observe in Figs. 7 a, for a duty cycle near 50%, there is no overvoltage on the drain (around 40 volt, half of $V_{ds_{max}}$), while converter output voltage equal to 125 volt. Nevertheless, we see on Fig. 7.a a non linear evolution of the source current (I_s) after 10 μ s of conduction implying a beginning of saturation in the inductor. This phenomena is not observed in Fig. 7.b for which we have increased the switching frequency.

During experiments, we have continuously checked the temperature of the various discrete elements of the circuits and we have not noticed any heating, even of the MOSFET. In fact, the recovery structure naturally involves a decrease of losses in the MOSFET, which don't need in consequence any cooler system. This confirms a better efficiency of the converter, compared with a basic boost converter in which a temperature increase of the switch was observed in the same operating conditions. The recovery of energy available at the opening of the transistor, which is the main improvement of this setup compared with the basic boost converter, is thus verified.

As for efficiency measurement, two versions of converter were experimented: without recovery diode (first improved Step-Up) and with (second improved Step-Up). For the two switching frequencies, 27 kHz and 47 kHz, we have recorded the efficiency as function of the nominal output power of the converter on a graph plotted in Fig. 8.

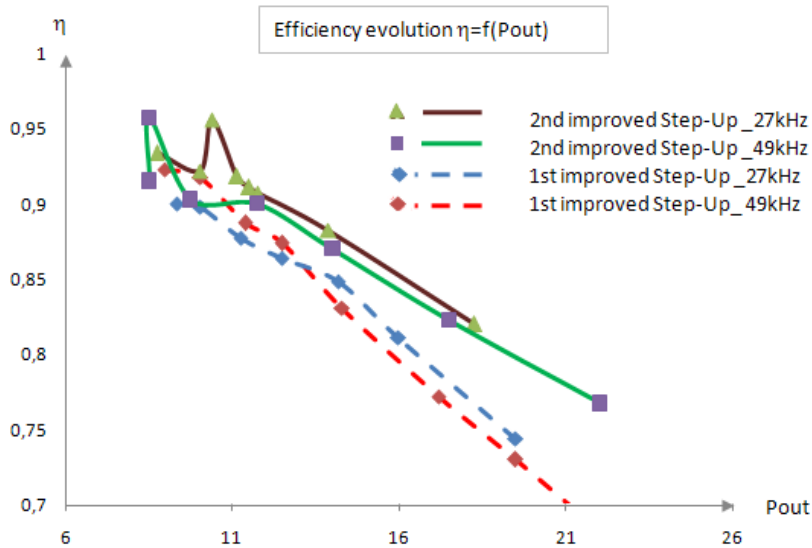


Fig. 8: Efficiency of the two versions of coupled-coils boost converter with two switching frequencies 27 kHz and 47 kHz.

In all experiments, we note a large decrease of the efficiency with the power. It confirms the non-linear model of the MOSFET submitted in another paper [4]. It is to be of note that the efficiencies presented in Fig. 8 are lower than the efficiencies observable in real applications due to the resistor used as current-voltage converter for the measurements. We also observe that the magnetically coupled boost converter with the recovery stage presents a better efficiency than the one's without, especially for high power.

In spite of an efficiency decrease with the power, these two circuits, and especially the converter with the recovery stage, show a real progress in the DC/DC high voltage conversion (output voltage above 100 volt for these first experiments). The behaviour of such converter can be optimized for higher power up to

180W (power of usual PV panels on the roofs with input voltage around 40 volt) and more by tuning the transformer and using nitrite carbide Schottky diodes.

Finally, all these measurements have been done in the same environment and with the same acquisition parameters, especially the current-voltage resistor. Some considerations were not taken into account during experiments, such as the very low coupling coefficient in the autotransformer which can be found in high voltage transformers. We can also imagine improve the experimental accuracy by the replacement of the resistor used for the current measurement by a Hall-Effect sensor, which is the least disruptive current-voltage converter.

3. Conclusion

The powerful conversion of high DC voltages from photovoltaic panels into a HVDC grid implicates simple, reliable, and cheap high efficiency converters while supplying voltages higher than 100V. These high voltage structures were considered until recently as a technological lock in classical Boosts. In the present study, we have shown by simulation and by measurement on electronic prototypes that the use of an autotransformer coupled with a recovery stage driven by a smart PWM control with a nominal duty cycle near 50% presents a real progress in term of efficiency compared to the basic boost converter dedicated to low power conversion. In this study, some experimental parameters slightly affect the obtained results, such as (i) the coupling coefficient in the autotransformer which is supposed equal to one and (ii) the current-voltage converter which introduces joules losses.

These systems need to be characterized more specifically to get higher output voltages than the first one experimented in this study.

Different versions of the two improved Step-Up boost converters will be tested with the individual connection of 12V and 40V PV panels to a grid able to supply a standard inverter. This architecture should allow to test and compare in real conditions energy harvest of converter integrated modules with the one produced by a conventional string, particularly in the case of partial shadowing, without forgetting to consider system safety risks such as arc fault prevention by diagnosis routines.

Acknowledgements

The authors gratefully acknowledge Institut Universitaire de Technologie de Thionville-Yutz, (IUT-TY, University of Lorraine) and particularly its director, Prof. J. Falla for the financially support and for the facilities offered during their researches.

References

- [1] Haeberlin H. and Graf J.D. Gradual Reduction of PV Generator Yield due to Pollution, 2nd World Conference on Photovoltaic Solar Energy Conversion, Vienna, Austria, 1998.
- [2] Woyte A., Nijs J., and Belmans R. Partial shadowing of photovoltaic arrays with different system configurations: literature review and field test results, Elsevier, Solar Energy 74, 2003, p. 217-233.
- [3] Walker G.R. and Sernia P.C. Cascaded DC-DC Converter Connection of Photovoltaic Modules, IEEE Trans on Power Electronics, vol 19, n°4, july 2004, p 1130-1139.
- [4] Petit P., Zegaoui A., Sawicki J.P., Aillerie M., Charles J.P. Rds(on) behavior in various MOSFET families, *IEEE Industr. Electron. ISIE 2011* DOI: 10.1109/ISIE.2011.5984184, 2011; 353-357.
- [5] Zhao Q. and Lee F.C. High-Efficiency High Step-Up DC–DC Converters, IEEE Trans. Power Electron. 18, 1 (2003).
- [6] Yi-Ping Hsieh, Jiann-Fuh Chen, Tsorng-Juu Liang, and Lung-Sheng Yang. A Novel High Step-Up DC-DC Converter for a Microgrid System. IEE Transactions on Power Electronics, vol.26, n°4, april 2011.